

Characterisation of Sn-Cl co-doped β -Ga₂O₃ thin films deposited via spray pyrolysis and their application in UV detector devices

Rakhy Raphael ^a, Sebin Devasia ^{a,b}, Sadasivan Shaji ^c, E.I. Anila ^{a,d,*}

^a Optoelectronics and Nanomaterials' Research Laboratory, Department of Physics, Union Christian College, Aluva, Kerala 683102, India

^b Nanotechnology - Research, Innovation and Incubation Centre (NRIC), PSG Institute of Advanced Studies, Coimbatore, Tamil Nadu 641004, India

^c Facultad de Ingeniería Mecánica y Eléctrica, Universidad Autónoma de Nuevo León, San Nicolás de los Garza, Nuevo León, Mexico

^d Department of Physics, CHRIST (Deemed to be University), Bengaluru, Karnataka 560029, India

ARTICLE INFO

Keywords:
Spray pyrolysis
UV detector
Thin films
Conductivity
Gallium oxide

ABSTRACT

Ga₂O₃, an ultrawide bandgap semiconducting oxide, is currently emerging as a promising candidate for various applications, such as power devices, solar-blind UV detectors, high temperature oxygen sensors and biomedical imaging. One significant limitation hindering the application of Ga₂O₃ as a wide-bandgap semiconductor is its poor conductivity. In this work, we investigate whether doping with tin and chlorine can mitigate this condition. Sn-Cl co-doped β -Ga₂O₃ thin films are deposited on glass substrates using spray pyrolysis technique. The deposited films are subjected to comprehensive analysis, including structural, optical and morphological measurements using techniques like X-ray diffraction, UV-Vis-NIR spectroscopy, X-ray photoelectron spectroscopy and EDX studies. Electrical properties are assessed using the four-probe method and Hall measurements. The best conductivity of $8.86 \Omega^{-1}m^{-1}$ is observed when 8.68 at% of Sn and 3.37 at% of Cl were co-doped into Ga₂O₃ (S (3)) and its optical band gap is calculated to be 4.65 eV. This is about five orders of improvement in conductivity as compared to that of pure Ga₂O₃ thin film deposited by the same method. Furthermore, we have constructed a deep UV detector utilizing doped β -Ga₂O₃ thin films as the semiconducting absorbing layer. The detector demonstrated the highest responsivity of $2.54 \times 10^{-4} A/W$ at 260 nm and the corresponding specific detectivity is 1.4×10^9 Jones. The current research validates the potential of Sn-Cl co-doped β -Ga₂O₃ thin film as an excellent choice for UV detector application.

1. Introduction

Recently, research reports on Ga₂O₃ reveal some interesting properties of the material, which makes it a competent material in the field of power electronics, UV detectors, transparent electronics, photocatalytic applications and luminescent applications [1–4]. Possessing an ultra-wide bandgap of 4.5 eV – 5 eV, Ga₂O₃ shows excellent sensitivity for UV light below 280 nm and is likely to be integrated in commercial UV detectors in near future [5,6]. UV detectors are generally employed for flame detection, defence applications, detection of biochemical reaction, underwater communication etc. As far as space applications are concerned, β -Ga₂O₃ demonstrates high radiation resistance comparable to that of GaN or SiC-based films. With very high critical breakdown field (8 MV/cm), and Baligas's figure of merit more than 3000, Ga₂O₃ is an attractive semiconductor for power applications compared to other materials Si, SiC and GaN [7,8]. Researchers are also exploring

luminescence, high temperature sensing, photocatalytic, bioimaging and antibacterial properties of Ga₂O₃ nanomaterial [8–11].

Although there are five different polymorph forms of Ga₂O₃, namely α , β , γ , ε and δ , β phase is especially interesting due to its unique properties [12]. Monoclinic β phase is the most stable phase with a direct band gap of nearly 4.8 eV. At high temperatures, other phases get naturally transformed to β phase. Monoclinic crystal lattice reveals two dissimilar positions for Ga atoms and three dissimilar positions for O atoms, namely Ga1, Ga2, O1, O2 and O3. Ga1 and Ga2 have tetrahedral and octahedral coordination with neighbouring oxygen atoms, respectively [13]. O1 is coordinated with four neighbouring atoms, whereas O2 and O3 are surrounded with three neighbouring atoms each. β -Ga₂O₃ crystal substrates are accessible in the market for epitaxial growth of different layers in manufacturing semiconductor devices [8]. Till date, thin films and nano powders of β -Ga₂O₃ are synthesized by variety of techniques including vacuum evaporation, hydrothermal method,

* Corresponding author at: Department of Physics, CHRIST (Deemed to be University), Bengaluru, Karnataka 560029, India.

E-mail address: anila.ei@christuniversity.in (E.I. Anila).

pulsed laser deposition and chemical vapour deposition [14–17]. In addition to these techniques, Ga_2O_3 thin films are fabricated by a few research groups using low cost, large area spray pyrolysis technique [18, 19]. Different coating parameters like substrate temperature, carrier pressure, solution flow rate, molarity of precursor solution are the key factors to be optimised in spray coating [4].

The main limitation in developing Ga_2O_3 based devices for commercial applications, is the poor conductivity of the material. As per previous research reports, undoped β - Ga_2O_3 exhibits intrinsic n-type conductivity due to presence of oxygen vacancies and gallium interstitials. The conductivity can be improved by introducing suitable dopants such as Ge, Sn, Si, Cl, H etc in thin films. Donor concentration was attained in a range between 1×10^{17} and $1 \times 10^{19} \text{ cm}^{-3}$ using various dopants. According to Simulation work done by Sun et. al. Sn substitutes Ga atoms while Cl can substitute either O or Ga atoms [8]. The substitution site is mainly determined based on the matching of ionic sizes [8]. Sn is a suitable dopant as it belongs to the fourteenth group and effectively donates one electron per atom when Sn is in 4+ state. Although tin has two main oxidation states, +2 and +4, in the Ga_2O_3 crystal, Sn^{4+} is more likely due to the similarity of the ionic radii of Ga^{3+} (62 ppm) and Sn^{4+} (52–81 ppm) ions. Sn^{2+} ions (118 ppm) have a radius comparably larger than that of Ga^{3+} ions [20]. Baldini et. al. reported MOVPE-deposition of Sn-doped β - Ga_2O_3 thin films on (010) β - Ga_2O_3 substrates [17]. Li et.al studied performance of UV detector using Sn-doped Ga_2O_3 films deposited by radio frequency magnetron sputtering [21]. Du et.al. deposited Sn-doped gallium oxide on β - Ga_2O_3 (100) substrates by metal organic chemical vapor deposition method [22]. Huang et.al. produced tin- gallium Oxide thin films by D C magnetron sputtering method [23].

While there are numerous research papers discussing Sn-doped β - Ga_2O_3 thin films deposited through different techniques, there is a lack of reported information on thin films deposited through spray methods. Additionally, the impact of Cl doping in β - Ga_2O_3 thin films has not been explored so far. In this context, we present the first report on the deposition of Sn-Cl co-doped β - Ga_2O_3 thin films using the spray pyrolysis method.

2. Experimental techniques

At first, the substrates underwent extensive cleaning, starting with ultrasonication in isopropanol, followed by rinsing in de-ionized water, and then drying in a hot air oven. Doped Ga_2O_3 thin films were deposited by spray pyrolysis technique using air as the carrier gas and optimal conditions obtained for coating pure Ga_2O_3 samples were selected [4]. For preparing precursor solution, 1.28 g of gallium nitrate hydrate [$\text{Ga}(\text{NO}_3)_3 \cdot x\text{H}_2\text{O}$, 99.9 %, Sigma Aldrich] was added to 50 ml distilled water by magnetic stirring [24]. Doping with tin was achieved by adding appropriate weight of Tin (II) Chloride dihydrate [$\text{SnCl}_2 \cdot 2\text{H}_2\text{O}$] to the above solution. The mass of the precursor (m) required for preparing X Molar, V ml solution was calculated using the formula.

$$m = \frac{XMV}{1000} \quad (1)$$

where M is the molecular mass. Four samples S (1), S (2), S (3) and S (4) were prepared, by incorporating Sn 5 at%, Sn 7.5 at%, Sn10 at% and Sn 12.5 at% in Ga_2O_3 thin films. As each $\text{SnCl}_2 \cdot 2\text{H}_2\text{O}$ molecule introduces 1 tin atom and 2 chlorine atoms to the crystalline lattice, concentration of chlorine is expected to be double that of tin. The precursor solution was deposited onto the glass substrates, arranged over the hot plate at 400°C . The spray flow rate and duration were set at 2 ml/min and 5 minutes respectively.

The structural characterisation of deposited thin film samples was analysed using Bruker AXS D8 Advance X-ray diffractometer with a Cu K α source. UV-Visible absorption and transmission studies were conducted using a Shimadzu UV-1900 spectrophotometer.

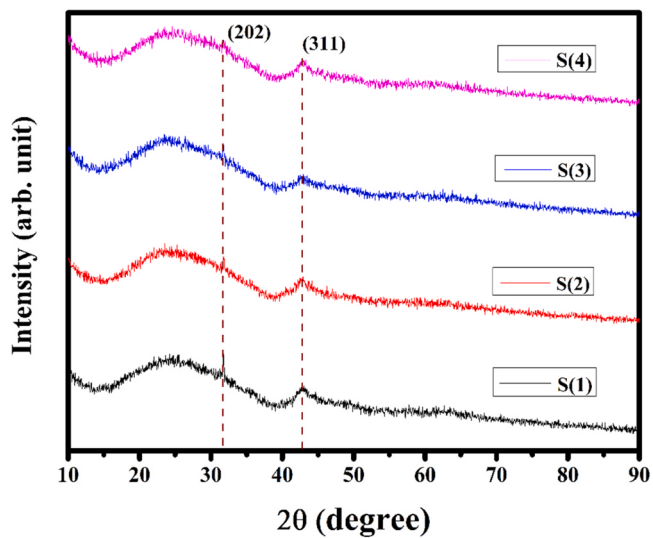


Fig. 1. XRD patterns of Ga_2O_3 thin films with different Sn and Cl concentrations.

Photoluminescence measurements were carried out using Fluoromax 4 C spectrofluorometer with a Xenon lamp source. The samples' chemical composition was examined through X-ray photoelectron spectroscopy measurements using the Thermoscientific K-alpha instrument. High magnification morphological images were captured using the field emission scanning electron microscope [FESEM] Thermoscientific Apero 2 SEM. For Hall measurements, Ecopia hms-3000 system was employed. Electrical conductivity was measured by the four-probe measurement technique using a Keithly 2450 source meter. The thickness of thin films is found to be 225 nm using Stylus profilometer.

3. Results and discussions

3.1. X-Ray diffraction (XRD)

In Fig. 1, XRD results of Ga_2O_3 thin films indicate that all samples are semicrystalline in nature. There are two low intensity peaks at 31.8° and 42.9° , that can be assigned to (202) and (311) planes of Ga_2O_3 respectively (ICDD PDF 00–041–1103). The intensity of the peaks gradually decrease as Sn concentration is elevated from 5 at% to 12.5 at%. The broad band extending from 15° to 40° originates due to the glass substrates. Even at doping percentage 12.5 at%, no additional peaks of SnO or SnO_2 are observed in the XRD pattern. Using Scherrer formula (1), grain size was calculated to be 4.6 nm, 4.2 nm, 4.1 nm, 5.3 nm for samples S(1), S(2), S(3) and S(4) respectively corresponding to the peak (311).

$$\text{Grain size} = \frac{0.9\lambda}{\beta \cos\theta} \quad (2)$$

3.2. UV –Visible transmission studies

Fig. 2(a) and (b) shows the effect of Sn and Cl doping on transmission percentage and band gap values of Ga_2O_3 thin film samples. Doped samples have transmission percentage greater than 80 % in the visible region. The transmission percentage is maximum for Sample S (1). For the other samples, S (2), S (3), and S (4), the transmission percentage is slightly lower than that of Sample S (1) and remains almost the same in the wavelength range of 450 nm to 700 nm.

The Tauc equation for direct band gap determination is given by

$$\alpha h\nu = A(h\nu - E_g)^{1/2} \quad (3)$$

where α is the optical absorption coefficient, $h\nu$ is the photon energy,

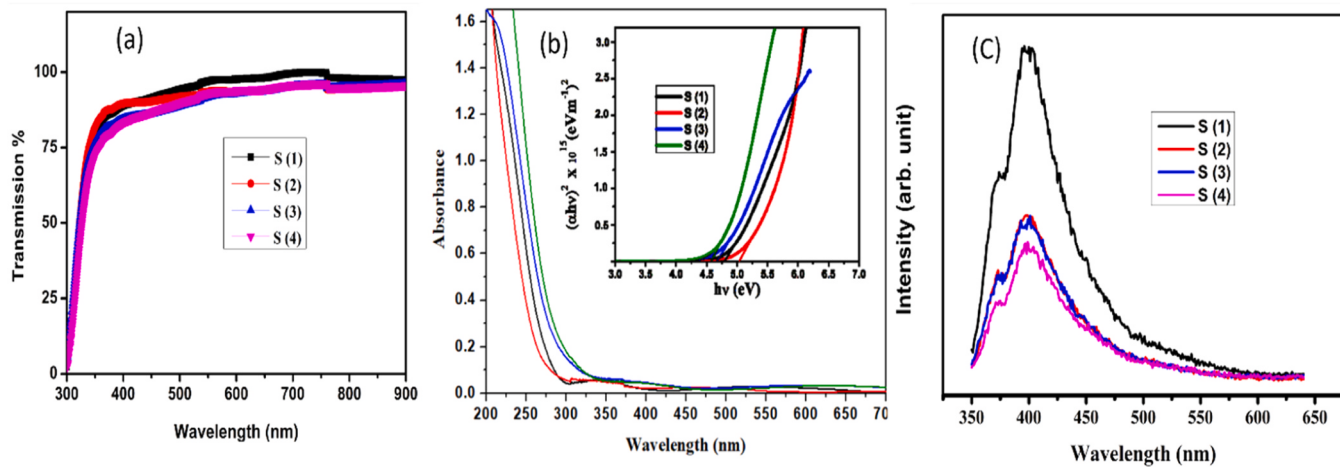


Fig. 2. a) Transmission percentage of Ga_2O_3 thin films with different dopant concentrations b) Tauc plot for band gap measurement c) photoluminescence spectra for Sn-Cl co-doped thin films.

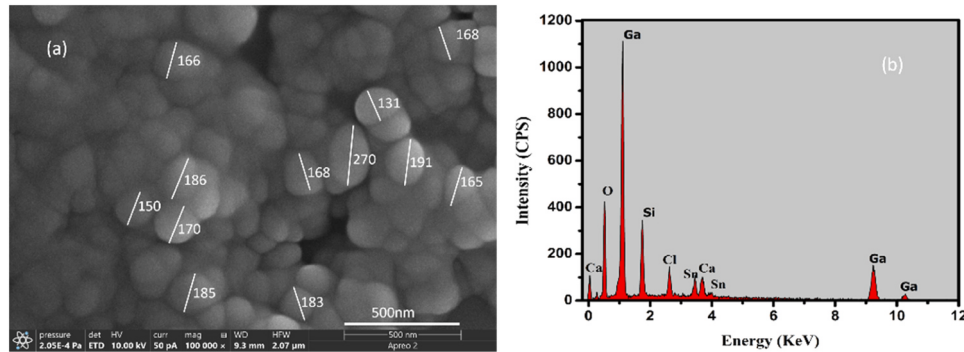


Fig. 3. a) FESEM image, b) EDX spectrum of S (3) sample.

E_g is the direct band gap and A is the proportionality constant. A graph is plotted between $(\alpha h\nu)^2$ versus $h\nu$, and by extrapolating the linear part to intersect the $h\nu$ axis, the band gap values are determined [25]. The band gap of Sn doped thin films exhibit irregular variations, with values determined as 4.85 eV, 5.12 eV, 4.65 eV, and 4.73 eV for S (1), S (2), S (3) and S (4) respectively in doped Ga_2O_3 thin films.

The underlying theory behind the fluctuation of the band gap is rather complicated and can be comprehended in the following manner. Various factors contribute to determining the band gap in these samples with doping. In pure β - Ga_2O_3 , the main contribution to the valence band edge comes from the O-2p orbitals, whereas the conduction band edge is mainly influenced by the Ga-4s orbitals. However, when tin is introduced, the process of hybridization becomes crucial in determining the alterations in the electronic structure. The band gap can be reduced due to the sp-d exchange interaction between the valence-band electrons and the localized d electrons of Sn [26,27]. In Sn-Cl doping, the band gap of the sample can increase due to the Burstein-Moss effect, as lower conduction band levels are occupied [28]. Hall measurements on the samples confirm an increase in carrier concentration for higher doping percentages, resulting in a higher band gap. However, dopants can also cause a band tailing effect, which reduces the band gap value [26]. The combined effect is observed in the present study, leading to nonuniform variation in band gap values. From S (1) to S (2), band gap increases due to BM shift, later for S (3) and S (4), band gap decreases due to enhancement in band tails, as no. of defect states are increased. During spray deposition, there is chance for Cl to escape from the solution and lesser percentage of Cl is present in the samples. Fluctuations in Cl concentration may also contribute to the variability in band gap values.

In 2c) Photoluminescence spectra of the samples exhibit two

emission peaks at 372 nm and 390 nm, which originate from host material Ga_2O_3 . Recombination of electrons trapped in Gallium vacancy sites, with holes in valence band give rise to these emissions [4]. Tin doping cause reduction in PL emission intensity, because tin occupies gallium vacancy sites and also defects cause energy emission in the form of nonradiative transitions.

3.3. Morphological and compositional analysis

In Fig. 3a, FESEM image of S (3) thin film reveals spherical agglomerated particles on the film with an average diameter of 180 nm. However, compared to the grain size calculated from XRD, the particle size appears significantly larger. In Fig. 3b, EDX spectra of samples reveal the presence of Ga, O, Sn, Cl, Si and Ca. The peaks corresponding to silicon and calcium are also observed in EDX spectrum due to their presence in glass substrate.

3.3.1. X-ray photoelectron spectroscopy (XPS)

The investigation of chemical composition using XPS, in Fig. 4, shows the presence of Ga, O, Sn and Cl in the spray deposited thin film sample. The Ga 2p_{3/2} and Ga 2p_{1/2} doublet peaks were observed at 1118.14 eV and 1144.98 eV with a spin-orbit splitting of 26.84 eV [29]. This can be assigned to the Ga³⁺ state in Ga_2O_3 thin films [30,31]. Correspondingly, O 1s peak was deconvoluted to obtain the major peak at 530.82 eV indicating the single oxidation state of metallic species in the thin films [3]. The additional low intensity peak observed at 532.5 eV represents the complex species (C-O and O-H bonds) formed by the adsorbed oxygen on the sample [3,31]. Further, the core-level spectrum of Sn 3d shows characteristic 3d_{5/2} and 3d_{3/2} peaks at

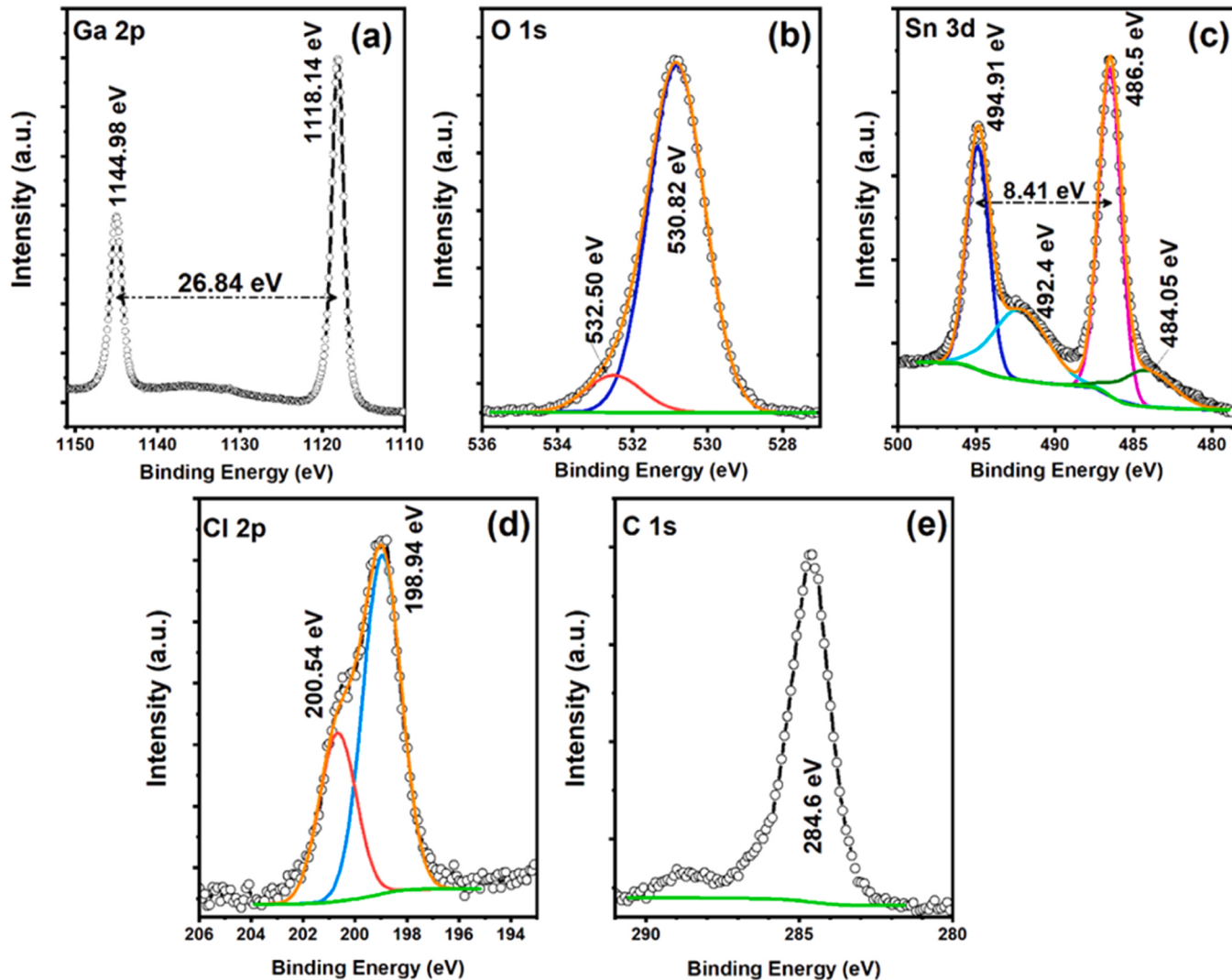


Fig. 4. The high-resolution XPS spectra of (a) Ga 2p, (b) O 1 s, (c) Sn 3d and (d) Cl 2p collected after a single Ar ion etching of the S (3) sample. (e) C 1 s spectrum of adventitious carbon used for the calibration.

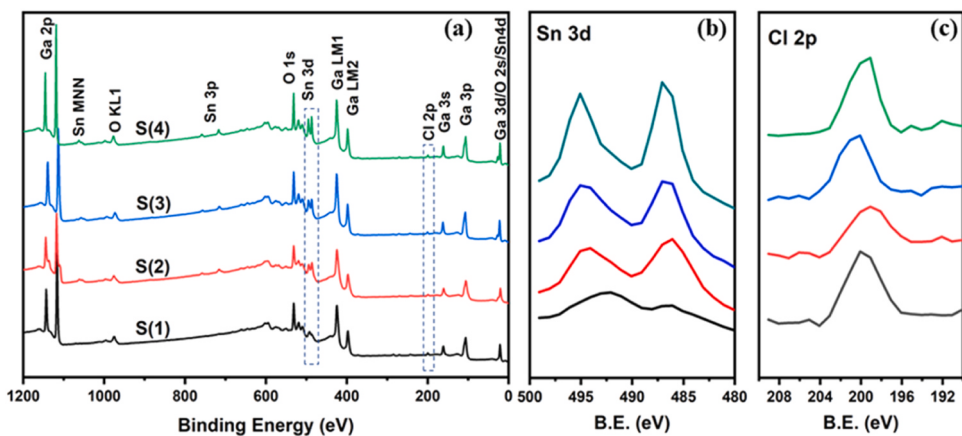


Fig. 5. (a) The survey spectrum of all the samples, collected after a single Ar ion etching, displays the presence of Sn and Cl in the sample. For a better clarity, the zoomed regions of (b) Sn 3d and (c) Cl 2p can be referred.

486.50 and 494.91 eV, respectively, with a binding energy difference of 8.41 eV that can be assigned to the Sn^{4+} states confirming its incorporation into Ga_2O_3 structure [3,29]. The Ar^+ ion etching results in the

SnO metallic states which corresponds to the 484.05 eV and 492.4 eV peaks in Fig. 1c [3]. In addition, the analysis reveals the presence of Cl in the sample which may be due to the precursor SnCl_2 used for Sn doping.

Table 1

The elemental composition estimated from the XPS survey spectrum.

Sample	Elemental composition (at%)			
	Ga 2 s	O 1 s	Sn 3d	Cl 2p
S (1)	32.02	59.50	4.42	4.06
S (2)	37.19	53.94	5.84	3.03
S (3)	35.12	52.82	8.68	3.37
S (4)	30.20	54.11	12.04	3.65

The Fig. 1d shows the doublet peaks Cl 2p_{3/2} and Cl 2p_{1/2} at 198.9 and 200.5 eV, respectively, with a binding energy difference of 1.6 eV [29]. This higher binding energy value as compared to the Cl in SnCl₂ (Cl 2p_{3/2} = 198.6 eV) corresponds to a higher oxidation state with the formation of Cl-O bonds [32].

Fig. 5 displays the survey spectra showing the presence of Sn and Cl in all the fabricated Ga₂O₃ samples. The low intense peaks observed here support and confirm the co-doping of Sn and Cl into the Ga₂O₃ crystal lattice. Additionally, Table 1 shows the elemental composition quantified from the XPS data using the CasaXPS software [33].

From Table 1, XPS analysis indicates that the atomic percentage of Cl in thin films does not show a consistent increase from S (1) to S (4). There is a possibility of Cl evaporation during spray deposition, leading to a reduction in Cl doping levels in the samples. Variations in Cl concentration can be reflected in the transmission and band gap values.

3.4. Electrical measurements

Hall measurements were carried out to identify semiconductor nature and to calculate the parameters conductivity, mobility and carrier concentration of different samples. Hall results confirm that all samples except S (4) have n type behaviour and conductivity rises gradually, as we increase tin and chlorine doping percentage. Table 1, summarize the obtained values of different thin film samples. For S (4) sample, we have not obtained reliable results. Conductivity is calculated also from four probe measurement results. Fig. 6 shows the relationship between voltage and current for the thin films that were deposited. From the

graph, resistivity (ρ) values are calculated and results are included in Table 2 for comparison.

$$\text{Resistivity of a thin film } \rho = \frac{4.53 \Delta V d}{\Delta I} \quad (4)$$

where d is the thickness of the film and $\frac{\Delta V}{\Delta I}$ is the reciprocal of the slope of the V-I characteristics. S (4) has conductivity value of $15.7 \Omega^{-1}\text{cm}^{-1}$, but voltage-current characteristics shows deviation from ohmic behaviour. With Sn and Cl co-doping, carrier concentration increases significantly, which leads to the improvement in the conductivity values. There is no appreciable variation in obtained mobility values for different samples. Compared to the conductivity value $8 * 10^{-5} \Omega^{-1}\text{cm}^{-1}$ of pure Ga₂O₃ thin film deposited by same method, Sn-Cl co-doping improves its value by five orders of magnitude [4]. The thin film sample S (3) exhibits the highest conductivity value among the samples. The results obtained in this study surpass those reported for (Ga₂O₃: Sn) films deposited using the MOCVD method [22].

As the conductivity value of S(3) is greater than that of other doped samples, it is used for developing a deep UV detector. Here doped Ga₂O₃ layer act as the UV light absorption layer, in which photoexcitation creates large number of free carriers, hence cause sudden rise in current. In our work, silver paste is employed for electrodes. Performance of the fabricated detector is analysed by placing it under a UV lamp (8 W), and measuring the current using the four probe arrangement connected to

Table 2

Summary of the values obtained from Hall measurement for different samples.

Sample	Conductivity ($\Omega^{-1}\text{cm}^{-1}$)	Mobility ($\text{cm}^2/\text{V s}$)	Carrier concentration ($/\text{cm}^3$)	Conductivity (Two-Probe method) ($\Omega^{-1}\text{cm}^{-1}$)
S (1)	$(2.81 \pm 0.07) * 10^{-3}$	(8.895 ± 1.8)	$(5.39 \pm 2.85) * 10^{15}$	$(7.24 \pm 0.04) * 10^{-3}$
S (2)	$(1.18 \pm 0.06) * 10^{-2}$	(22.18 ± 5.35)	$(1.76 \pm 0.86) * 10^{17}$	$(1.25 \pm 0.03) * 10^{-2}$
S (3)	(8.86 ± 0.11)	(16.39 ± 0.31)	$(3.73 \pm 0.17) * 10^{18}$	$(8.70 \pm 0.52) * 10^{-1}$

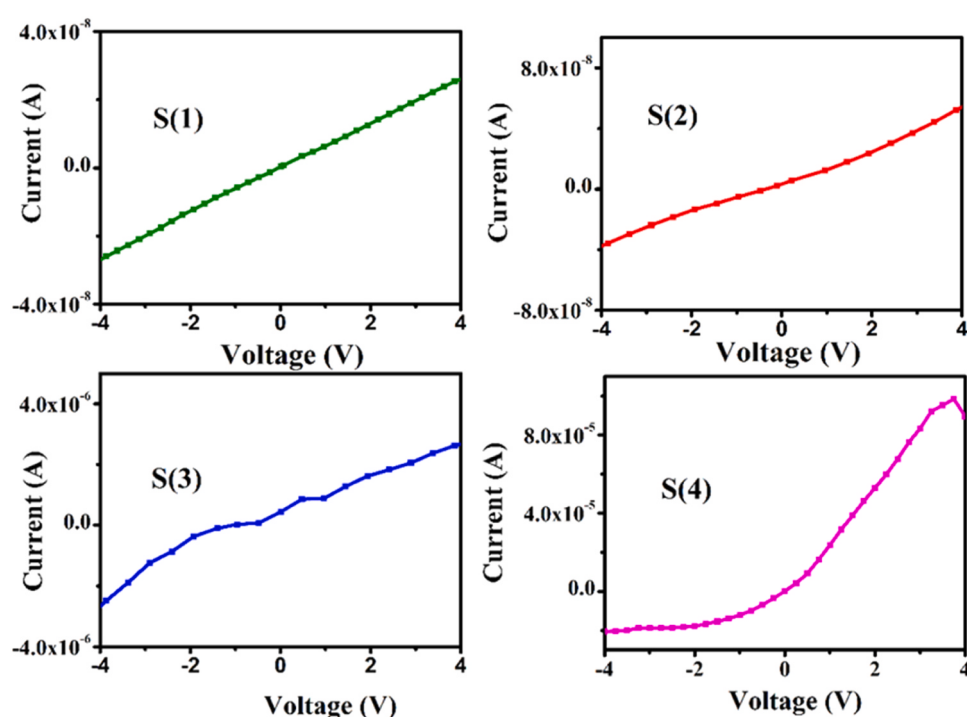


Fig. 6. Graph of Current Vs Voltage for different Sn-Cl co-doped Ga₂O₃ samples.

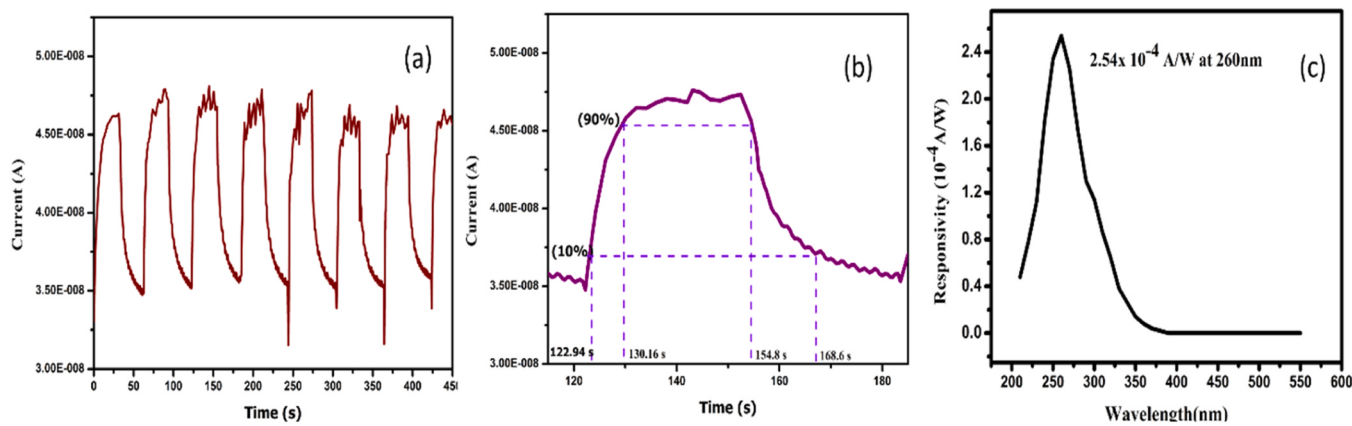


Fig. 7. a) and b) Time response c) spectral response of the UV detector constructed using S (3) sample.

Keithly 2450 source meter. The bias voltage was kept at 10 V and current is measured under both dark and light conditions. UV lamp was switched on and off with an interval of 60 s and from time response (fig:7), growth and decay constants are calculated as 7.2 s and 13.8 s respectively [34].

The performance parameters of the detector such as responsivity, specific detectivity, external quantum efficiency and sensitivity were evaluated using the equations given below.

$$\text{Responsivity}, \quad (R) = \frac{I_{\text{light}} - I_{\text{dark}}}{I_0 A} \quad (5)$$

$$\text{Specific detectivity}, \quad (D) = \frac{R\sqrt{A}}{\sqrt{2e}I_{\text{dark}}} \quad (6)$$

$$\text{Sensitivity}, \quad (S) = \frac{I_{\text{light}} - I_{\text{dark}}}{I_{\text{dark}}} X 100 \quad (7)$$

Here I_{light} and I_{dark} symbolize current measured under light and dark conditions and A indicate the area of the detector exposed to light. The fabricated detector has responsivity, specific detectivity, and sensitivity as 2.54×10^{-4} A/W, 1.4×10^9 Jones and 37 respectively at wavelength 260 nm.

4. Conclusions

Spray deposited, Sn-Cl double doped Ga_2O_3 thin films were studied using different material characterisation techniques. X-ray diffraction studies reveal faint low intensity peaks of $\beta\text{-Ga}_2\text{O}_3$. Band gap of the thin films is found to be ranging from 4.65 eV to 5.12 eV. Electrical studies confirm that tin doping helps to improve conductivity of Ga_2O_3 thin film. Highest conductivity value was obtained for S (3), which is desirable for deep UV detector application. A UV detector was fabricated with sample S (3) and performance parameters such as responsivity, specific detectivity, and sensitivity were obtained as 2.54×10^{-4} A/W, 1.4×10^9 Jones and 37 respectively at wavelength 260 nm.

CRediT authorship contribution statement

Anila E I: Supervision, Methodology. **Rakhy Raphael:** Writing – original draft, Investigation, Conceptualization. **Sadasivan Shaji:** Resources. **Sebin Devasia:** Resources, Formal analysis.

Declaration of Competing Interest

The authors declare that they have no known competing financial interests or personal relationships that could have appeared to influence the work reported in this paper.

Data availability

Data will be made available on request.

References

- [1] S.J. Pearson, J. Yang, P.H. Cary, F. Ren, J. Kim, M.J. Tadjer, M.A. Mastro, A review of Ga_2O_3 materials, processing, and devices, *Appl. Phys. Rev.* 5 (1) (2018) 011301, <https://doi.org/10.1063/1.5006941>.
- [2] S.R. Thomas, G. Adamopoulos, Y.H. Lin, H. Faber, L. Sygellou, E. Stratikakis, N. Pliatsikas, P.A. Patsalas, T.D. Anthopoulos, High electron mobility thin-film transistors based on Ga_2O_3 grown by atmospheric ultrasonic spray pyrolysis at low temperatures, *Appl. Phys. Lett.* 105 (9) (2014) 092105 <https://doi.org/10.1063/1.4894643>.
- [3] S. Ghose, S. Rahman, L. Hong, J.S. Rojas-Ramirez, H. Jin, K. Park, R. Klie, R. Dronpaad, Growth and characterization of $\beta\text{-Ga}_2\text{O}_3$ thin films by molecular beam epitaxy for deep-UV photodetectors, *J. Appl. Phys.* 122 (9) (2017) 095302, <https://doi.org/10.1063/1.4985855>.
- [4] R. Raphael, S. Devasia, S. Shaji, E.I. Anila, Effect of substrate temperature on the properties of spray deposited Ga_2O_3 thin films, for solar blind UV detector applications, *Opt. Mater.* 133 (2022) 112915, <https://doi.org/10.1016/j.optmat.2022.112915>.
- [5] Z. Ji, J. Du, J. Fan, W. Wang, Gallium oxide films for filter and solar-blind UV detector, *Opt. Mater.* 28 (4) (2006) 415–417, <https://doi.org/10.1016/j.optmat.2005.03.006>.
- [6] J. Xu, W. Zeng, F. Huang, Gallium oxide solar-blind ultraviolet photodetectors: a review, *J. Mater. Chem. C.* 7 (2019) 8753–8770, <https://doi.org/10.1039/C9TC02055A>.
- [7] Priyanshi Goyal, Harsupreet Kaur, Impact of dual material gate design and retrograde channel doping on $\beta\text{-Ga}_2\text{O}_3$ MOSFET for high power and RF applications, *Silicon* 15 (2022) 1–12, <https://doi.org/10.1007/s12633-022-02079-7>.
- [8] D. Sun, Y. Gao, J. Xue, J. Zhao, Defect stability and electronic structure of doped $\beta\text{-Ga}_2\text{O}_3$: a comprehensive ab initio study, *J. Alloy. Compd.* 794 (2019) 374–384, <https://doi.org/10.1016/j.jallcom.2019.04.253>.
- [9] I.A. Hassan, S. Sathasivam, H.U. Islam, C.J. Carmalt, $\text{Ga}_2\text{O}_3\text{-Cu}_2\text{O}$: synthesis, characterisation and antibacterial properties, *RSC Adv.* 7 (2017) 551–558, <https://doi.org/10.1039/C6RA24737G>.
- [10] K. Girija, S. Thirumalairajan, D. Mangalaraj, Morphology controllable synthesis of parallelly arranged single-crystalline $\beta\text{-Ga}_2\text{O}_3$ nanorods for photocatalytic and antimicrobial activities, *Chem. Eng. J.* 236 (2014) 181–190, <https://doi.org/10.1016/j.cej.2013.09.088>.
- [11] N. Vorobyeva, M. Rumyantseva, V. Platonov, D. Filatova, A. Chizhov, A. Marikutsa, I. Bozhev, A. Gaskov, $\text{Ga}_2\text{O}_3\text{(Sn)}$ oxides for high-temperature gas sensors, *Nanomaterials* 11 (11) (2021) 2938, <https://doi.org/10.3390/nano11112938>.
- [12] A.K. Saikumar, S.D. Nehate, K. Sundaram, Review—RF sputtered films of Ga_2O_3 , *ECS J. Solid State Sci. Technol.* 8 (2019) Q3064, <https://doi.org/10.1149/2.0141907jss>.
- [13] S. Geller, Crystal Structure of $\beta\text{-Ga}_2\text{O}_3$, *J. Chem. Phys.* 33 (1960) 676, <https://doi.org/10.1063/1.1731237>.
- [14] H.J. Bae, T.H. Yoo, Y. Yoon, I.G. Lee, J.P. Kim, B.J. Cho, High-aspect ratio $\beta\text{-Ga}_2\text{O}_3$ nanorods via hydrothermal synthesis, *Nanomaterials* 8 (8) (2018) 594, <https://doi.org/10.3390/nano8080594>.
- [15] A.K. Saikumar, S.D. Nehate, K.B. Sundaram, Review—RF sputtered films of Ga_2O_3 , *ECS J. Solid State Sci. Technol.* 8 (2019) Q3064–Q3078, <https://doi.org/10.1149/2.0141907jss>.
- [16] A. Mahmoodinezhad, C. Janowitz, F. Naumann, P. Plate, H. Gargouri, K. Henkel, D. Schmeißer, J.I. Flege, Low-temperature growth of gallium oxide thin films by plasma-enhanced atomic layer deposition, *J. Vac. Sci. Technol. A* 38 (2020) 022404, <https://doi.org/10.1116/1.5134800>.

- [17] M. Baldini, M. Albrecht, A. Fiedler, K. Irmscher, R. Schewski, G. Wagner, Editors' Choice—Si- and Sn-doped homoepitaxial β -Ga₂O₃ layers grown by MOVPE on (010)-oriented substrates, *ECS J. Solid State Sci. Technol.* 6 (2017) Q3040, <https://doi.org/10.1149/2.0081702jss>.
- [18] S.R. Thomas, G. Adamopoulos, Y.H. Lin, H. Faber, L. Sygellou, E. Stratakis, N. Pliatsikas, P.A. Patsalas, T.D. Anthopoulos, High electron mobility thin-film transistors based on Ga₂O₃ grown by atmospheric ultrasonic spray pyrolysis at low temperatures, *Appl. Phys. Lett.* 105 (2014) 092105, <https://doi.org/10.1063/1.4894643>.
- [19] N. Winkler, R.A. Wibowo, W. Kautek, G. Ligorio, E.J.W. List-Kratochvil, T. Dimopoulos, Nanocrystalline Ga₂O₃ films deposited by spray pyrolysis from water-based solutions on glass and TCO substrates, *J. Mater. Chem. C* 7 (2019) 69–77, <https://doi.org/10.1039/c8tc04157a>.
- [20] Y. Zhang, J. Yan, G. Zhao, W. Xie, First-principles study on electronic structure and optical properties of Sn-doped b-Ga₂O₃, *Phys. B: Phys. Condens. Matter B* 405 (2010) 3899–3903, <https://doi.org/10.1016%2Fj.physb.2010.06.024>.
- [21] L. Li, C. Li, S. Wang, Q. Lu, Y. Jia, H. Chen, Preparation of Sn-doped Ga₂O₃ thin films and their solar-blind photoelectric detection performance, *J. Semicond.* 44 (2023) 062805, <https://doi.org/10.1088/1674-4926/44/6/062805>.
- [22] X. Du, Z. Li, C. Luan, W. Wuang, Preparation and characterization of Sn-doped β -Ga₂O₃ homoepitaxial films by MOCVD, *Journal of Materials Science* 50(8) 3252–3257, <https://doi.org/10.1007/s10853-015-8893-4>.
- [23] Y. Huang, Z. Ji, C. Chen, Preparation and characterization of p-type transparent conducting tin-gallium oxide films, *Appl. Surf. Sci.* 253 (2007) 4819–4822, <https://doi.org/10.1016/j.apsusc.2006.10.043>.
- [24] C.C. Pye, A. Hendsbee, K.D. Nizio, B.L. Goodall, J.P. Ferguson, J.D. Masuda, J.A. C. Clyburne, The thermal decomposition of gallium nitrate hydrate, Ga(NO₃)₃·9H₂O, *Polyhedron* 197 (2021), <https://doi.org/10.1016/j.poly.2021.115040>.
- [25] S.S. Abdullahi, S. Güner, Y. Koseoglu, I.M. Musa, B.I. Adamu, M.I. Abdulhamid, Simple method for the determination of band gap of a nanopowdered sample using Kubelka Munk theory, *J. Niger. Assoc. Math. Phys.* 35 (2016) 241–246.
- [26] G.G. Nicolas, Synthesis and characterization of Tin (Sn) incorporated GA₂O₃, Open Access Theses Diss. 3417 (2021). (https://scholarworks.utep.edu/open_etd/3417).
- [27] W. Mi, X. Du, C. Luan, H. Xiao, J. Ma, Electrical and optical characterizations of β -Ga₂O₃: Sn films deposited on MgO (110) substrate by MOCVD, *RSC Adv.* 4 (2014) 30579–30583, <https://doi.org/10.1039/C4RA02479F>.
- [28] E. Burstein, Anomalous Optical Absorption Limit in InSb, *Phys. Rev.* 93, 632–633, <https://doi.org/10.1103/PhysRev.93.632>.
- [29] J.F. Moulder, W.F. Stickle, P.E. Sobol, K.D. Bomben, *Handbook of X-ray photoelectron spectroscopy: a reference book of standard spectra for identification and interpretation of XPS data*, Perkin-Elmer Corporation, USA, 1992 <https://doi.org/9780962702624>.
- [30] T. Chowdhury, XPS Depth Profile Study of Sprayed Ga₂O₃ Thin Films, *Engineering* 15 (2023) 459–466, <https://doi.org/10.4236/eng.2023.158035>.
- [31] R. Saha, S. Bhowmick, M. Mishra, A. Sengupta, S. Chattopadhyay, S. Chakrabarti, Impact of deposition temperature on crystalline quality, oxygen vacancy, defect modulations and hetero-interfacial properties of RF sputtered deposited Ga₂O₃ thin films on Si substrate, *J. Phys. D: Appl. Phys.* 55 (2022) 505101, <https://doi.org/10.1088/1361-6463/ac9b69>.
- [32] R. Félix, N. Llobera-Vila, C. Hartmann, C. Klimm, M. Hartig, R.G. Wilks, M. Bär, Preparation and in-system study of SnCl₂ precursor layers: towards vacuum-based synthesis of Pb-free perovskites, *RSC Adv.* 8 (2018) 67–73, <https://doi.org/10.1039/C7RA12172E>.
- [33] N. Fairley, V. Fernandez, M. Richard-Plouet, C. Guillot-Deudon, J. Walton, E. Smith, D. Flahaut, M. Greiner, M. Biesinger, S. Tougaard, D. Morgan, J. Baltrusaitis, Systematic and collaborative approach to problem solving using X-ray photoelectron spectroscopy, *Appl. Surf. Sci. Adv.* 5 (2021) 100112, <https://doi.org/10.1016/JAPSADV.2021.100112>.
- [34] J. Mathew, E.I. Anila, Hydrothermal assisted chemical bath deposition of (Cd:Zn)S thin film with high photosensitivity and low dark current, *Sol. Energy* 172 (2018) 165–170, <https://doi.org/10.1016/j.solener.2018.05.075>.

Dr. E I Anila is a Professor at CHRIST (Deemed to be University) located in Bangalore, Karnataka, India. She earned her Ph.D. from Cochin University of Science and Technology, Kerala, India. Prior to her tenure at CHRIST, Dr. Anila served as a Professor at Union Christian College in Kerala, India. Her expertise and passion lie in the realm of nanomaterials, specifically focusing on their applications in optoelectronics, biomedicine, energy storage, and environmental remediation. Driven by a profound commitment to innovative research, she explores the multifaceted potentials of nanomaterials to address crucial challenges in various domains.

Rakhy Raphael is an assistant professor at Department of Physics, U C College, Aluva, Kochi, Kerala. She is currently doing PhD at ONRL lab, U C College, affiliated to M G University under the guidance of Dr. E.I. Anila. Her research interests include transparent conducting oxides, nanophosphors, optoelectronic devices and U V detector.

Dr. Sebin Devasia serves as an Assistant Professor of Physics at the esteemed PSG Institute of Advanced Studies in Coimbatore. With a profound dedication to materials research, he endeavors to propel the realm of advanced semiconductor thin films, particularly in the domains of photovoltaics, photodetectors, and various optoelectronic applications. Dr. Sebin's primary focus lies in the exploration of perovskite and lead-free perovskite-inspired materials, delving deep into their intricate light-matter interactions. Additionally, he employs state-of-the-art computational calculations grounded in density functional theory (DFT) to unveil the intricate electronic and optical properties inherent in semiconductor materials.

Dr. Sadasivan Shaji, is a distinguished Professor at the Universidad Autonoma de Nuevo Leon, Mexico, specializes in nanomaterials and their applications in solar cells and thin films. His research encompasses laser ablation in liquids, optoelectronic properties of nanomaterials, and the synthesis and characterization of nanomaterials using advanced techniques such as TEM, SEM, DRX, XPS, and Raman spectroscopy. Dr. Shaji's recent contributions include pioneering work on ultraviolet to near infrared wavelength-independent photodetectors and the development of lead-free thin films for visible light photodetection. He plays a pivotal role in institutional development through his leadership in the Laboratory for Synthesis of Nanomaterials by Laser Ablation and his involvement in national research projects.